Ponds on Eros: Pert NEAR but not plumb?

James Roberts[1*], Olivier Barnouin[1], Eliezer Kahn[1], Louise Prockter[1], Carolyn Ernst[1], and Bob Gaskell[2]

[1]Johns Hopkins University Applied Physics Laboratory, [2]Planetary Science Institute, *Email: James.Roberts @jhuapl.edu

The apparent distribution of small ponds on Eros may reflect an observational bias. A significant fraction of ponds do not have flat floors.

Poster Number 136-7

1. Introduction

NEAR-Shoemaker Multi-Spectral Imager (MSI) data reveal more than 300 "ponds" on asteroid 433 Eros: **smooth deposits** that sharply embay the bounding depressions in which they lie, and whose spectra appear **blue** relative to that of the surrounding terrain [1-5]. An example is shown in Figure 1.

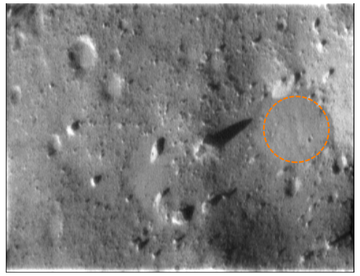

Figure 1: An example of a pond candidate located at 184.0°E, 2.95 °S in MSI Image 155888731. Pond (outlined by the dashed circle) is 75 m in diameter. The deposits appear smoother and finer-grained than the surroundings.

Here we investigate the apparent distribution of ponds on Eros and compare this to the distribution of image pixel scales as a function of location on the asteroid, using a shape model derived from stereo analysis [2,5] of MSI data. **We also investigate the topography of these ponds** using a shape model derived from stereophotoclinometric analysis [6], and validated against altimetry from the NEAR Laser Rangefinder (NLR; [7]). We update the locations of 55 pond candidates identified in images registered to the new shape model. **We classify the flatness of these features** according to the behavior of the first and second derivatives of the topography. We use our results to **constrain the mode of pond formation** from among existing hypotheses [1,2,8].

2. Origin Hypotheses

We examine three general hypotheses for the formation of ponded deposits:

1. The pond material originates from regolith surrounding local depressions. These materials are then transported to and sequestered in the bottoms of depressions by **seismic shaking** caused by impacts elsewhere on Eros [1].
2. The result of the accumulation of the finest components of regolith by **electrostatic levitation** [2], transported to and trapped within a bounding depression [9].
3. Many of the ponds could be the result of **disaggregating boulders** commonly observed in their midst, broken up either by micrometeorites or thermal cracking [8].

Both hypotheses 2 and 3 anticipate subsequent seismic shaking is [2,8] in order to distribute the pond material onto an equipotential.

3. Pond Distribution

- **Ponds concentrated at equatorial latitudes, near long ends of asteroid**
- Gravity is lowest here – promotes electrostatic levitation? [2]
- Near terminator a lot – thermal fatigue in boulders? [8]
- **NEAR was closest to Eros at these locations.**
  - We map ponds on shape model using the **Small Body Mapping Tool** (SBMT)
    - Interactive 3D visualization tool developed at the Johns Hopkins University Applied Physics Laboratory (JHU/APL) [10]
    - Available through a public JHU/APL website (http://sbmt.jhuapl.edu)
- Strong correlation between distribution of ponds and high image pixel scale (Figs. 2-4) [11].

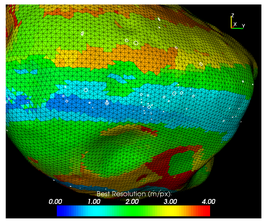

Figure 2: Map of plate scale on Eros, centered at 7°S, 11°W. Ponds are shown as white circles superimposed on the shape model.

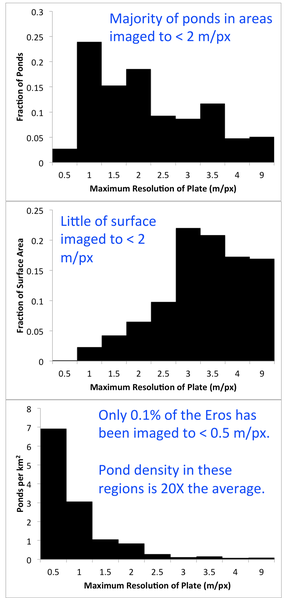

Figure 3: Histograms showing the distribution of ponds as a function of the best imaging pixel scale at the pond location (top); the distribution of the surface area of Eros imaged and modeled at a given pixel scale (middle); and the number of ponds found per square km in each pixel scale bin. (bottom)

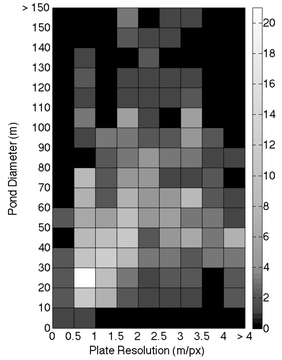

Figure 4: 2D histogram showing the distribution of ponds as a function of image pixel scale and pond diameter

- 60% of ponds in locations that have been imaged to better than 2.0 m/px, comprising only 13% of the surface area of Eros [11].
- We have attempted to find known ponds seen in coarser pixel scale images than the ones in which they were originally identified (Figure 5).
- Even large (D > 100 m) known ponds are difficult to find in coarse pixel-scale (> 5 m/px) images [11].
  - Virtually impossible without *a priori* knowledge of their location from the higher-resolution images.
- **May be many more unidentified small ponds in coarse pixel-scale areas.**

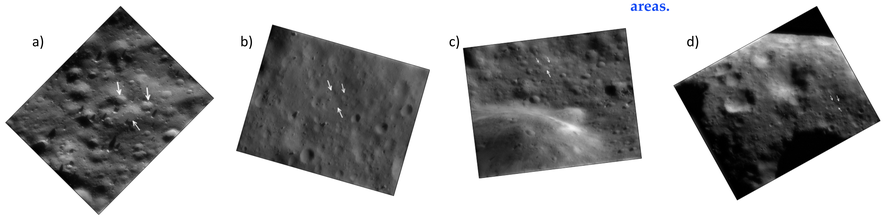

Figure 5: Four images containing a distinctive group of ponds (166-168) at a range of pixel scales. a) MSI 152448816 (1.9 m/px). b) MSI 135533146 (3.5 m/px). c)MSI 147076129 (5.1 m/px). d)MSI 131112663 (8.8 m/px). All images are rotated to place north at the top. The ponds form a distinctive pattern with the smaller two forming an east-west line to the north of the larger pond. The ponds lie just to the east of a north-south trending chain of craters, which provides context for locating the area.

4. Pond Topography

Topography can be classified according to the behavior of its first and second derivatives:

- **Level**: The slope is low or zero, indicating that the pond elevation is at a local minimum.
- **Flat**: The Laplacian is low or zero, indicating that the slope does not vary with position.

A pond whose surface follows an equipotential should satisfy both criteria. Furthermore, **a flat-floored pond should have an obvious break in slope** between the flank and floor, In contrast, a bowl-shaped depression has a gradually-varying slope throughout.

The floors of many ponds do not appear to be flat. The elevation, slopes and Laplacians for Ponds 28 and 86 are shown in Figure 6. Topographic profiles through these ponds are shown in Figure 7. Pond 28 appears to be flat; pond 86 has an extremely high Laplacian at the point where the slope is lowest, suggesting the floor is not flat [12].

Of the 55 ponds we have examined, only 24 have clearly flat floors with a break in slope at the edges.

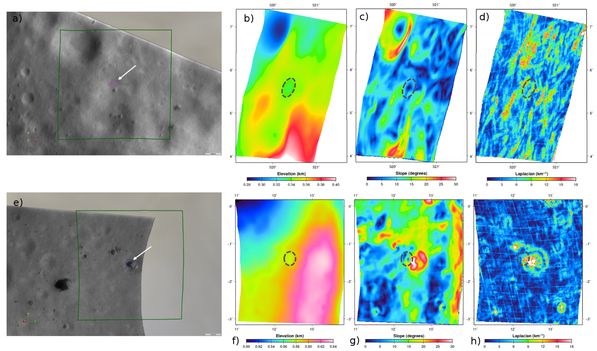

Figure 6: MSI Images (a,e); elevation with respect to gravity (b,f), slope (c,g), and Laplacian (d,h) of two pond candidates. Pond 28 (a-d) exhibits a low Laplacian co-incident with the center of the pond, surrounded by a ring, indicating a break in slope. Pond 86 (e-h) is dominated by a large central boulder. The pond is emplaced on a steep background slope; thus, the lowest point is offset to the west (downslope) of the boulder. The Laplacian is high at the center of the pond, suggesting the absence of a flat floor. Ponds are outlined in dark gray.

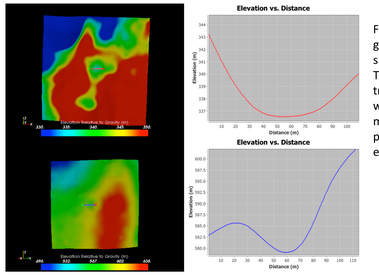

Figure 7: Elevation with respect to gravity for ponds 28 and 86 with sample transects shown (left). Topographic profiles along the transects (right). Pond 28 shows a well-flattened floor. Pond 86 appears more bowl-shaped, suggesting that the pond material is not lying on an equipotential.

5. Altimetry

- Improve topographic analysis by incorporating NLR altimetry
- Data in NLR track are extremely accurate with respect to each other
- Sparse coverage -- only a few ponds contain NLR tracks
- Entire track may be offset from actual location due to errors in spacecraft pointing
- We rigidly translate entire NLR track to shape model (Figures 8 and 9)
- Agrees with SPC to within a few meters

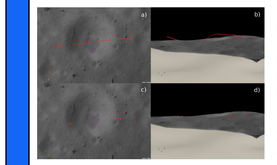

Figure 8: Example of the NLR shift. Face-on (left) and oblique (right) views of MSI image 139820288 projected onto the Gaskell [6]) shape model. A magenta circle indicates the location of Pond candidate 87 (appears edge on in panels b and d). An NLR track is shown in red before (top) and after a rigid translation (bottom) to minimize misfit between the perceived NLR location and the shape model.

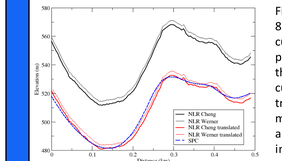

Figure 9: Elevation over Pond Candidate 87, as measured by the NLR (solid black curves) using two different reference potentials, and as computed based on the SPC-derived shape model (dashed curve). The red curves represent a rigid translation of the NLR topography to minimize the misfit between altimetry and the shape model arising from errors in the NEAR-Shoemaker trajectory estimation.

6. Conclusions

1. **Strong correlation between distribution of ponds and regions of best image pixel scale.**
   - Apparent pond distribution probably has observational bias at small (< 30 m) scales.
   - Should not be used to discriminate among formation hypotheses.
2. **Only 45% of ponds have clearly flat floors with break in slope at edges.**
3. Does not support *in situ* origin of ponds material.
   - Erosion of central boulder should lead to more obvious break in slope.
   - Electrostatic levitation possible if material adheres to slopes.
   - Seismic shaking possible, material may not settle to equipotential.
4. Good agreement between NLR and SPC (< 2m) after translation.

References: [1] Cheng, A. F., et al. (2002), *MAPS* 37, 1095-1105. [2] Robinson, M. S., et al. (2001), *Nature* 413, 396-400. [3] Veverka, J., et al. (2001), *Science*, 292, 484-488. [4] Cheng, A. F., et al. (2001), *Science* 292, 484-488. [5] Thomas, P. C., et al. (2002), *Icarus* 155, 18-37. [6] Gaskell, R. W., et al. (2008), *MAPS* 43, 1049-1061. [7] Zuber, M. T., et al. (2001), *Science* 289, 2097-2101. [8] Dombard, A. J., et al. (2010) *Icarus* 210, 713-721. [9] Hughes, A. L. H. et al. (2008), *Icarus* 195, 630-648. [10] Kahn, E. G., et al. (2011), *LPSC* 42, 1618. [11] Roberts, J. H. et al. (2014), *Icarus* 241, 160-164. [12] Roberts, J. H. et al. (2014), *MAPS* 49, 1735-1748.